Asian Journal of Chemistry; Vol. 29, No. 4 (2017), 896-904

ASIAN JOURNAL OF CHEMISTRY

https://doi.org/10.14233/ajchem.2017.20356

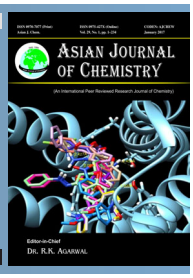

Pro-Apoptotic Activity of Novel 4-Anilinoquinazoline Derivatives Mediated by Up-Regulation of Bax and Activation of Poly(ADP-ribose) Phosphatase in Ehrlich Ascites Carcinoma Cells

PREETHI SALIGRAMA DEVEGOWDA[1], KYATHEGOWDANADODDI SRINIVAS BALAJI[2], DODDAKUNCHE SHIVARAMU PRASANNA[3], TORESHETTAHALLY RAMESH SWAROOP[4], SHANKAR JAYARAMA[2], LOKESH SIDDALINGAIAH[1,*] and KANCHUGARAKOPPAL SUBBEGOWDA RANGAPPA[5,*]

[1]Department of Studies in Biotechnology, University of Mysore, Manasagangotri, Mysore-570 006, India
[2]Department of Biotechnology, Teresian College, Siddarthanagar, Mysore-570 011, India
[3]Department of Nanotechnology, Visvesvaraya Technological University, Center for Postgraduate Studies, Bengaluru Region, Muddenahalli, Chikkaballapur District-562 101, India
[4]Department of Studies in Organic Chemistry, University of Mysore, Manasagangotri, Mysore-570 006, India
[5]Department of Studies in Chemistry, University of Mysore, Manasagangotri, Mysore-570 006, India

*Corresponding authors: E-mail: boramma@rediffmail.com; rangappaks@yahoo.com

Received: 18 October 2016; *Accepted*: 27 December 2016; *Published online*: 31 January 2017; AJC-18269

Quinazolines are very important class of heterocyclic compounds with antitumor properties. In search of novel anti-tumour agents, a series of 4-anilinoquinazolines were synthesized and characterized using proton and ^{13}C NMR, Fourier transform infrared and mass spectroscopic techniques. These compounds were evaluated for their cytotoxic effect on ehrlich ascites carcinoma cells using MTT assay. Among the tested compounds, compound N-(3-((6,7-dimethoxyquinazoline-4-yl)amino)phenyl)-4-nitrobenzene sulfonamide exhibited more potent activity with an IC_{50} value of 10.29 ± 1.14 µM against ehrlich ascites carcinoma cell line. *in vivo* studies using compound N-(3-((6,7-dimethoxyquinazoline-4-yl)amino)phenyl)-4-nitrobenzene sulfonamide (**4G**) showed that there was reduction in the mice body weight, ascites volume and decrease in cell number. Mice treated with compound **4G** showed higher survivability compared with that of control mice. The cells treated with compound **4G** also exhibited typical morphological changes of apoptotic damages. Further, compound **4G** induced tumour cell death by activating pro-apoptotic protein Bax which activates caspase-3 which in turn cleaves poly (ADP- ribose) polymerase and causes DNA fragmentation. Thus, our results strongly conclude that our compound **4G** acts as a antincancer agent by inducing apoptosis in ehrlish ascites carcinoma cells.

Keywords: Quinazoline, Ehrlich ascites carcinoma cells, Apoptosis.

INTRODUCTION

Apoptosis is referred as programmed cell death [1]. It plays a crucial role in normal development and tissue homeostasis by facilitating the removal of unwanted, damaged or infected cells [1,2]. Impairment of the apoptotic signal promotes aberrant cell proliferation, agglomeration of genetic defects, ultimately resulting in tumorigenesis [3]. Therefore, induction of apoptosis in cancer cells is a target for developing potent antineoplastic drug in cancer treatment. It is an energy dependent process in which the characteristic morphological changes occur, it includes plasma membrane blebbing, exposure of phosphatidylserine at the external surface of the cell membrane, cell shrinkage, chromatin condensation and DNA fragmentation [3,4].

At the molecular level, apoptosis is tightly regulated by the activation of the aspartate-specific cysteine protease (caspase) cascade. Activation of caspase cascade can be initiated through activation of the apoptotic pathway [5]. The distinguished extrinsic and intrinsic apoptotic pathway is based on the involvement of adaptor molecules and initiator caspases. These two pathways are interlinked and the molecules in one pathway influence the other pathway [6]. The mitochondrial pathway is regulated by activating pro-apoptotoic proteins Bax and inhibiting the anti-apoptotic proteins Bcl_2 of the Bcl-2 family [7-9]. Cellular stress induces pro-apoptotic protein Bax to migrate to the surface of the mitochondria, where it procreate pores in the mitochondrial membrane and permit the release of cytochrome C into cytoplasm. Once cytochrome C is released, it activates intiator caspases-9 and results in the cleavage of effector caspase -3, -6 and -7 [7,8,10]. The active caspase-3 and -7 specifically cleaves poly (ADP-ribose) polymerase (PARP) that will lead to the nucleosomal DNA fragmentation [11,12]. Cleavage of a definite number of key proteins is very important for the development of apoptotic events.

Quinazolines are big family of heterocyclic compounds, which have shown broad variety of biological activity profiles, such as analgesic [13], diuretic, antihypertensive [14], antimalarial [15], antibiotic, antitumoral [16-18], antiangiogenic [19] and many others. It is observed that the biological activity strongly depends on the type and the place of the substituents in their molecules. Even though various substitutions can be made on quinazoline ring, 4-amino substituted quinazolines are used as anticancer, antifungal, anti-inflammatory, antihypertensive and antimicrobial agents [20-22]. Few of the 4-anilinoquinazolines have found to be potential and highly selective inhibitors of human immunoglobulin and epidermal growth factor receptor tyrosine kinase. Although the first signal transduction kinase inhibitor to proceed to clinical deployment was the pyrimidine derivative imatinib. Many investigations have employed quinazoline derivatives, with 4-anilino derivatives being particularly dominant in this regard. Quinazolines are reported as inhibitors of EGFR auto-phosphorylation [22] and the production of TNF-α [23].

In search of more potent molecules, we synthesized a series of novel quinazoline derivatives and evaluated those compounds for their antitumor property and identified some potent molecules for detailed studies.

EXPERIMENTAL

Experimental methodology and characterization data of synthesized quinazoline derivatives 4(A-J): The key intermediate compound 6,7-dimethoxy-quinazolin-4(3*H*)one (**1**) compound was synthesized using the earlier reported procedure [24].

Synthesis of 6,7-dimethoxy-4-chloro quinazoline (2): To a stirred solution of compound **1** (10 mmol) in thionyl chloride (3 mL), DMF was added (2-3 drops) slowly. The reaction mixture was heated to reflux and stirred for about 2 h. Excess thionyl chloride was distilled off and the reaction mixture was quenched in ice with efficient stirring. The precipitate was filtered, washed with ice-water and the crude material was dissolved in chloroform and filtered to remove insoluble impurities. Organic layer was concentrated under vacuum to obtain compound **2**.

Synthesis of N-(3-aminophenyl)-6,7-dimethoxy-quinazolin-4-amine (3): To a stirred solution of compound **2** (10 mmol) in isopropyl alcohol (25 mL) *meta*-phenylenediamine was added (10 mmol). The reaction mass was heated to 60 °C and stirred for about 3-4 h. Reaction was monitored by TLC. After completion, the reaction mass was quenched in ice water and sodium bicarbobnate and extracted with ethyl acetate. Organic layer was concentrated under vacuum to obtain compound **3**. The obtained crude product was purified by column chromatography to get pure compound **3**.

General procedure for the preparation of compounds 4(A-J): To a stirred solution of compound **3** (1 mmol) and triethyl amine (1 mmol) in dichloromethane (10 mL), aryl sulfonyl chlorides (1 mmol) at 0 °C was added. The reaction mixture was stirred and allowed to attain room temperature and continued stirring at room temperature for about 4-5 h. Completion of the reaction was monitored by TLC. The reaction mass was quenched with water and extracted to dichloromethane. The organic layer was dried over sodium sulphate and concentrated to obtain crude material. Further purification was done by column chromatography to get pure material of title compounds **4(A-J)** with yields ranging from 55 to 75 %.

N-(3-((6,7-Dimethoxyquinazoline-4-yl)amino)phenyl)-4-fluorobenzene sulfonamide (4A): White solid; m.p.: 168-170 °C. IR (KBr, ν_{max}, cm^{-1}): 3416, 3210, 1609. ^{1}H NMR (DMSO-d_6, 400 MHz) δ: 10.41 (s, 1H, -NH), 9.62 (s, 1H, -NH), 8.53 (s, 1H, Ar-H), 8.22 (s, 1H, Ar-H), 7.94 (s, 1H, Ar-H), 7.80 (m, 1H, Ar-H), 7.61 (m, 2H, Ar-H), 7.55 (m, 2H, Ar-H), 7.47 (m, 2H, Ar-H), 7.20 (m, 1H, Ar-H), 3.97 (s, 3H, -OCH_3), 3.95 (s, 3H, -OCH_3). ^{13}C NMR (DMSO-d_6, 100 MHz) δ: 168.4, 166.0, 158.6, 154.6, 151.3, 146.6, 143.2, 137.5, 135.3, 130.5, 130.2, 115.6, 112.9, 109.4, 108.2, 107.8, 102.7, 99.4, 56.2, 56.0. MS (ESI + ion): *m/z* = 454.8 Anal. calcd. for $C_{22}H_{19}N_4O_4SF$: C 58.14, H 4.21, N 12.33. Found: C 58.20, H 4.28, N 12.39.

N-(3-((6,7-dimethoxyquinazoline-4-yl)amino)phenyl)-4-methoxybenzene sulfonamide (4B): White solid; m.p.: 162-164 °C. IR (KBr, ν_{max}, cm^{-1}): 3430, 3222, 1602, 1315. ^{1}H NMR (DMSO-d_6, 400 MHz) δ: 10.39 (s, 1H, -NH), 9.57 (s, 1H, -NH), 8.47 (s, 1H, Ar-H), 8.24 (s, 1H, Ar-H), 7.97 (s, 1H, Ar-H), 7.84 (m, 1H, Ar-H), 7.12 (s, 1H, Ar-H), 7.59 (d, J= 8.0 Hz, 2H, Ar-H), 7.54 (d, J=8.0 Hz, 2H, Ar-H), 7.49 (m, 1H, Ar-H), 7.26 (d, 1H, Ar-H), 3.97 (s, 3H, -OCH_3), 3.93 (s, 3H, -OCH_3). ^{13}C NMR (DMSO-d_6, 100 MHz) δ: 168.4, 163.7, 158.4, 154.5, 151.2, 146.5, 143.1, 137.4, 132.0, 130.3, 126.0, 114.6, 112.9, 109.4, 108.2, 107.6, 102.7, 99.3, 56.2, 56.0, 55.8. MS (ESI + ion): *m/z* = 467.2. Anal. calcd. for $C_{23}H_{22}N_4O_5S$: C 59.22, H 4.75, N 12.01. Found: C 59.28, H 4.79, N 12.06.

2,5-Dichloro-N-(3-((6,7-dimethoxyquinazoline-4-yl)amino)phenyl)benzene sulfonamide (4C): White solid; m.p.: 178-180 °C. IR (KBr, ν_{max}, cm^{-1}): 3438, 3198, 1596, 1285. ^{1}H NMR (DMSO-d_6, 400 MHz) δ: 10.36 (s, 1H, -NH), 9.57 (s, 1H, -NH), 8.46 (s, 1H, Ar-H), 8.27 (s, 1H, Ar-H), 7. 96 (s, 1H, Ar-H), 7.64 (m, 2H, Ar-H), 7.59 (m, 1H, Ar-H), 7.50 (m, 2H, Ar-H), 7.45 (m, 1H, Ar-H), 7.21 (m, 1H, Ar-H), 3.96 (s, 3H, -OCH_3), 3.93 (s, 3H, -OCH_3). ^{13}C NMR (DMSO-d_6, 100 MHz) δ: 168.4, 158.5, 154.6, 151.3, 146.6, 143.2, 141.1, 137.5, 133.4, 132.7, 130.5, 130.3, 129.5, 128.0, 112.9, 109.4, 108.2, 107.8, 102.7, 99.4, 56.2, 56.0. MS (ESI + ion): *m/z* = 506.0. Anal. calcd. for $C_{22}H_{18}N_4O_4SCl_2$: C 52.29, H 3.59, N 11.09. Found: C 52.35, H 3.63, N 11.14.

4-Chloro-(3-((6,7-dimethoxyquinazoline-4-yl)amino)-phenyl)benzene sulfonamide (4D): White solid; m.p.: 174-176 °C. IR (KBr, ν_{max}, cm^{-1}): 3428, 3215, 1588, 1278. ^{1}H NMR (DMSO-d_6, 400 MHz) δ: 10.40 (s, 1H, -NH), 9.58 (s, 1H, -NH), 8.51 (s, 1H, Ar-H), 8.25 (s, 1H, Ar-H), 7.97 (s, 1H, Ar-H), 7.82 (m, 1H, Ar-H), 7.61 (m, 2H, Ar-H), 7.55 (d, J=8.0 Hz, 2H, Ar-H), 7.47 (d, *J* = 8.0 Hz, 2H, Ar-H), 7.20 (m, 1H, Ar-H), 3.97 (s, 3H, -OCH_3), 3.95 (s, 3H, -OCH_3). ^{13}C NMR (DMSO-d_6, 100 MHz) δ: 168.4, 158.5, 154.6, 151.3, 146.6, 143.2, 137.8, 137.5, 137.3, 130.3, 129.0, 128.6, 112.8, 109.4, 108.2, 107.8, 102.7, 99.4, 56.2, 56.0. MS (ESI + ion): *m/z* = 470.8. Anal. calcd. for $C_{22}H_{19}N_4O_4SCl$: C 56.11, H 4.07, N 11.90. Found: C 56.16, H 4.14, N 11.95.

4-(*tert*-Butyl)-N-(3-((6,7-dimethoxyquinazolin-4-yl)amino)phenyl)benzene sulphonamide (4E): White solid;

m.p.: 154-156 °C. IR (KBr, ν_{max}, cm^{-1}): 3432, 3219, 1595, 1289. ^{1}H NMR (DMSO-d_6, 400 MHz) δ: 10.41 (s, 1H, -NH), 9.56 (s, 1H, -NH), 8.49 (s, 1H, Ar-H), 8.22 (s, 1H, Ar-H), 7.95 (s, 1H, Ar-H), 7.80 (m, 1H, Ar-H), 7.61 (m, 2H, Ar-H), 7.52 (d, J=8.0 Hz, 2H, Ar-H), 7.44 (d, J=8.0 Hz, 2H, Ar-H), 7.18 (d, 1H, Ar-H), 3.97 (s, 3H, -OCH_3), 3.95 (s, 3H, -OCH_3), 1.32(s, 9H, -($C(CH_3)_3$)). ^{13}C NMR (DMSO-d_6, 100 MHz) δ: 168.4, 158.5, 154.5, 151.3, 146.6, 143.2, 137.5, 136.6, 130.3, 128.1, 125.4, 112.8, 109.3, 107.0, 108.2, 107.8, 102.7, 99.4, 56.2, 56.0, 34.2, 31.3. MS (ESI + ion): *m/z* = 493.0. Anal. calcd. for $C_{26}H_{28}N_4O_4S$: C 63.40, H 5.73, N 11.37. Found: C 63.45, H 5.78, N 11.42.

N-(3-((6,7-Dimethoxyquinazoline-4-yl)amino)phenyl)-2-nitrobenzene sulphonamide (4F): White solid; m.p.: 182-184 °C. IR (KBr, ν_{max}, cm^{-1}): 3441, 3227, 1581, 1283. ^{1}H NMR (DMSO-d_6, 400 MHz) δ: 10.41 (s, 1H, -NH), 9.56 (s, 1H, -NH), 8.47 (s, 1H, Ar-H), 8.26 (s, 1H, Ar-H), 8.19 (s, 1H, Ar-H), 7.97 (s, 1H, Ar-H), 7.84 (d, J=8.0 Hz, 2H, Ar-H), 7.76 (s, 1H, Ar-H), 7.62 (m, 1H, Ar-H), 7.46 (m, 2H, Ar-H), 7.39 (m, 1H, Ar-H), 3.99 (s, 3H, -OCH_3), 3.96 (s, 3H, -OCH_3). ^{13}C NMR (DMSO-d_6, 100 MHz) δ: 168.4, 158.5, 154.6, 151.2, 147.1, 146.5, 143.2, 137.5, 135.1, 134.4, 132.8, 130.3, 128.2, 124.2, 112.9, 109.4, 108.2, 107.8, 102.7, 99.4, 56.2, 56.0. MS (ESI + ion): *m/z* = 481.7. Anal. calcd. for $C_{22}H_{19}N_5O_6S$: C 54.88, H 3.98, N 14.55. Found: C 54.93, H 4.04, N 14.61.

N-(3-((6,7-Dimethoxyquinazoline-4-yl)amino)phenyl)-4-nitrobenzene sulphonamide (4G): White solid; m.p.: 196-198 °C. IR (KBr, ν_{max}, cm^{-1}): 3449, 3235, 1585, 1288. ^{1}H NMR (DMSO-d_6, 400 MHz) δ: 10.43 (s, 1H, -NH), 9.60 (s, 1H, -NH), 8.53 (s, 1H, Ar-H), 8.22 (s, 1H, Ar-H), 7.94 (s, 1H, Ar-H), 7.82 (m, 1H, Ar-H), 7.63 (d, J=8.0 Hz, 2H, Ar-H), 7.54 (m, 2H, Ar-H), 7.45 (d, J=8.0 Hz, 2H, Ar-H), 7.23 (m, 1H, Ar-H), 3.96 (s, 3H, -OCH_3), 3.94 (s, 3H, -OCH_3). ^{13}C NMR (DMSO-d_6, 100 MHz) δ: 168.4, 158.5, 154.6, 151.3, 151.1, 146.6, 145.8, 143.2, 137.5, 130.3, 128.2, 124.2, 112.9, 109.4, 108.2, 107.8, 102.7, 99.4, 56.2, 56.0. MS (ESI + ion): *m/z* = 481.7. Anal. calcd. for $C_{22}H_{19}N_5O_6S$: C 54.88, H 3.98, N 14.55. Found: C 54.94, H 4.06, N 14.60.

N-(3-((6,7-Dimethoxyquinazoline-4-yl)amino)phenyl)-3-nitrobenzene sulfoamide (4H): White solid; m.p.: 190-192 °C. IR (KBr, cm^{-1}): 3452, 3231, 1596, 1293. ^{1}H NMR (DMSO-d_6, 400 MHz) δ: 10.39 (s, 1H, -NH), 9.57 (s, 1H, -NH), 8.46 (s, 1H, Ar-H), 8.23 (s, 1H, Ar-H), 8.11 (s, 1H, Ar-H), 7.93 (s, 1H, Ar-H), 7.81 (m, 2H, Ar-H), 7.77 (s, 1H, Ar-H), 7.56 (m, 1H, Ar-H), 7.43 (m, 2H, Ar-H), 7.49 (m, 1H, Ar-H), 3.97 (s, 3H, -OCH_3), 3.94 (s, 3H, -OCH_3). ^{13}C NMR (DMSO-d_6, 100 MHz) δ: 168.4, 158.5, 154.6, 151.3, 148.3, 146.6, 143.2, 140.6, 137.5, 133.4, 130.3, 129.9, 127.1, 123.1, 112.9, 109.4, 108.2, 107.8, 102.7, 99.4, 56.2, 56.0. MS (ESI + ion): *m/z* = 481.7. Anal. calcd. for $C_{22}H_{19}N_5O_6S$: C 54.88, H 3.98, N 14.55. Found: C 54.92, H 4.02, N 14.58.

N-(3-((6,7-Dimethoxyquinazoline-4-yl)amino)phenyl)-benzenesulfonamide (4I): White solid; m.p.: 148-150 °C. IR (KBr, ν_{max}, cm^{-1}): 3456, 3241, 1602, 1282. ^{1}H NMR (DMSO-d_6, 400 MHz) δ: 10.33 (s, 1H, -NH), 9.53 (s, 1H, -NH), 8.44 (s, 1H, Ar-H), 8.21 (s, 1H, Ar-H), 8.12 (s, 1H, Ar-H), 7.93 (s, 1H, Ar-H), 7.82 (d, J=8.0 Hz, 2H, Ar-H), 7.74 (s, 1H, Ar-H), 7.60 (m, 2H, Ar-H), 7.40 (m, 2H, Ar-H), 7.33 (m, 1H, Ar-H), 3.98 (s, 3H, -OCH_3), 3.94 (s, 3H, -OCH_3). ^{13}C NMR (DMSO-d_6, 100 MHz) δ: 168.4, 158.5, 154.6, 151.3, 146.6, 143.2, 139.7, 137.5, 131.9, 130.3, 129.0, 127.3, 112.8, 109.4, 108.2, 107.8, 102.7, 99.4, 56.2, 56.0. MS (ESI + ion): *m/z* = 436.7. Anal. calcd. for $C_{22}H_{20}N_4O_4S$: C 60.54, H 4.62, N 12.84. Found: C 60.59, H 4.66, N 12.89.

N-(3-((6,7-Dimethoxyquinazoline-4yl)amino)phenyl)-2,3,5-trimethylbenzene sulphonamide (4J): White solid; m.p.: 166-168 °C. IR (KBr, cm^{-1}): 3466, 3239, 1608, 1277. ^{1}H NMR (DMSO-d_6, 400 MHz) δ: 10.36 (s, 1H, -NH), 9.57 (s, 1H, -NH), 8.46 (s, 1H, Ar-H), 8.27 (s, 1H, Ar-H), 7. 96 (s, 1H, Ar-H), 7.64 (m, 2H, Ar-H), 7.59 (s, 1H, Ar-H),7.50 (s, 1H, Ar-H), 7.45 (m, 1H, Ar-H), 7.21 (m, 1H, Ar-H), 2.38-2.42 (s, 9H, Ar-CH_3), 3.96 (s, 3H, -OCH_3), 3.93 (s, 3H, -OCH_3). ^{13}C NMR (DMSO-d_6, 100 MHz) δ: 168.3, 158.4, 154.5, 151.3, 146.6, 143.2, 138.7, 137.5, 137.0, 135.6, 134.0, 132.3, 130.3, 123.6, 112.9, 109.4, 108.2, 107.8, 102.7, 99.4, 56.2, 56.0, 21.6, 19.2, 19.1. MS (ESI + ion): *m/z* = 479. Anal. calcd. for $C_{25}H_{26}N_4O_4S$: C 62.74, H 5.48, N 11.71. Found: C 62.79, H 5.52, N 11.76.

Experimental procedure for biological assays: Swiss albino mice were procured from the central animal facility, Department of studies in Zoology, University of Mysore, Mysore, India. Ehrlich ascites carcinoma (EAC) cells were obtained from NCCS (Pune).

Antiproliferative assay: All the newly synthesized compounds **4(A-J)** were preliminarily evaluated for their antiproliferative activity on EAC cell lines using MTT assay [25]. Ehrlich ascites carcinoma cell lines (Mouse mammary carcinoma) were cultured in modified eagle's medium (MEM), supplemented with 10 % FBS at 37 °C and humidified atmosphere containing 5 % CO_2. Cells were seeded at a density of 1×10^4 cells/well in a 96 well plate and allowed to attach for 24 h. The media was removed and treated with different concentrations (1-100 µg) of compound for 24 h. Then, 10 µL of MTT solution (5 mg/mL) was added to each well and incubated at 37 °C for 4 h. Then, medium was removed and 200 µL of dimethyl sulfoxide was added to each well in order to solubilize formazan crystals. The absorbance was measured at 570 nm by micro plate reader. The IC_{50} value was defined as the concentration that caused 50 % inhibition of cell proliferation.

***in vivo* Treatment of compound 4G:** Ehrlich ascites carcinoma (5×10^6 cells/mouse) cells were injected intraperitonially into six to eight weeks old Swiss albino mice and the animals showed a significant increase in the body weight over the growth period. To determine, whether the compound inhibit tumor growth, compound **4G** (100 mg/kg) was administered into the EAC bearing mice on every alternate day starting from 6^{th} day of inoculation. The growth of tumor was monitored by taking the body weight every day. The animals were sacrificed on 11^{th} day. The volume of ascites from both treated and control were noted. The other group animals were used to study the survivability after treatment until their death [26].

Studies on cell morphology: Giemsa and nuclear staining were performed and visualized using light and fluorescent (Leitz-DIAPLAN) microscope. Both compound **4G** treated and untreated cells were harvested from mice, fixed in methanol: acetic acid (3:1) and were smeared on glass slide and air-dried in humidified chamber. The cells were hydrated with PBS and

stained with Giemsa or mixture of (1:1) acridine orange-ethidium bromide (4 µg/mL). These cells were washed with PBS and visualized under light or Leitz-DIAPLAN fluorescent microscope respectively [27-29].

Measurement of cell viability: *in vivo* treated and untreated cells were harvested from mice and the packed cells were diluted (1:6 ratio). Cell viability was assessed by counting the number of viable cells using haemocytometer by 0.4 % trypan blue dye exclusion method. Cells that picked up the dye were considered to be dead [26].

Apoptosis assay by FACS: Phycoerythrin conjugated antibody against activated caspase-3 (CloneC92-605) was used to label caspase-3 according to the manufacturer's instructions (BD Pharmingen); samples were analyzed by flow cytometry. Briefly, the cells were harvested from compound **4G** treated and control group, where in cisplatin was used as positive control. Then the cells were re-suspended in BD Cytofix/Cytoperm solution (BD Pharmingen) and incubated on ice for 20 min. The cells were washed with 1X BD Perm/Wash buffer (BD Pharmingen) and labelled with phycoerythrin- conjugated anti-activated caspase-3 antibody at room temperature for 30 min before analysis by flow cytometry (Beckman Coulter Inc) [30].

DNA fragmentation assay: This is a technique, which is used to visualize the endonuclease cleavage of apoptosis [31,32]. This assay involves extraction of DNA from treated and untreated cells using phenol-chloroform method. Cells were lysed using 10 % SDS, incubated for 30 min at 37 °C. The cell lysate was precipitated using 8 M potassium acetate at 4 °C for 1 h. The supernatant was extracted by phenol: choloroform:isoamyl alcohol (25:24:1). DNA was precipitated by adding 1:2 volume of ice-cold ethanol to the supernatant and was dissolved in TE buffer. The DNA was treated with RNase at 37 °C for 1 h. The extracted DNA was separated by 1.2 % agarose gel electrophoresis and visualized by staining with ethidium bromide under UV trans illuminator and documented using UVP-BioDoc-ItTM system.

Caspase-3 inhibition assay: Ehrlich ascites carcinoma cells harvested from control mice were pre-incubated with or without caspase-3 inhibitor AC-DEVE CHO (100 µM) at 37 °C for 1 h. Subsequently the cells were treated with compound **4G** and incubated for another 2 h at 37 °C. DNA was isolated and the fragmentation was visualized by 1.5 % agarose gel electrophoresis [30].

RNA isolation and reverse transcription-polymerase chain reaction: Total RNA from control and test sample was prepared using the Trizol reagent (Invitrogen) according to the manufacturer's protocol. 1 µg of RNA was reverse transcribed using the Super-Script III One-Step RT-PCR system (Invitrogen) [33,34]. Briefly, the complementary DNAs were synthesized at 50 °C for 30 min followed by incubation at 94 °C for 2 min. Subsequently, 30 cycles of PCR were carried out with denaturation at 94 °C for 45 seconds, annealing at 53 °C for 45 seconds and extension at 72 °C for 1.5 min, followed by a final incubation at 72 °C for 7 min. For amplifying Bax and Bcl-2 the following primers sets (Sigma) were used. Bax PCR primers set (Product No. B8304) Reverse primer sequence (3' antisense): 5'-CAT CTT CTT CCA GAT GGT GA-3' Forward primer sequence (5' sense): 5'-GTT TCA TCC AGG ATC GAG CAG-3' and Bcl-2 PCR primers set (Product No. B9179) Reverse primer sequence (3' antisense): 5'-GAG ACA GCC AGG AGA AAT CA-3' Forward primer sequence (5' sense): 5'-CCT GTG GAT GAC TGA GTA CC-3'. GAPDH (Product No. P7732) Reverse primer sequence (3' antisense): 5'-**Y**GC CTG CTT CAC CAC CTT C-3' Forward primer sequence (5' sense): 5'-TGC **M**TC CTG CAC CAC CAA CT-3' where **M** = A or C , **Y** = T or C that was used as a loading control, was amplified using primers that have been previously published. The PCR products were then separated on a 1.5 % agarose gel and results were documented.

Western blotting: Ehrlich ascites carcinoma cells treated and untreated with **4G** compounds were harvested and lysed for 1 h at 4 °C in lysis buffer (20 mM Tris pH 7.5, 2 mM EDTA, 3 mM EGTA, 2 mM dithiothreitol (DTT), 250 mM sucrose, 0.1 mM phenylmethylsulfonyl fluoride, 1 % Triton X-100) containing a protease inhibitor cocktail. Protein (50 µg) was resolved on 12.5 % SDS gel and transferred to PVDG membrane. Equal protein loading was controlled by Ponceau Red staining of membranes. For immunoblotting, anti-PARP (ab-72805) primary antibody was used followed by the addition of HRP-conjugated specific secondary antibody. Actin (ab-3280) was used as internal loading control. The protein bands were developed and visualized by enhanced chemiluminescence [35,36].

RESULTS AND DISCUSSION

The synthesis of quinazoline derivatives **4(A-J)** was carried out as per synthetic procedure represented in **Scheme-I**. The key intermediate compound 6,7-dimethoxy-quinazolin-4(3*H*)-one (**1**) was prepared using the earlier reported procedure. Compound **1** was treated with thionyl chloride in presence few drops of DMF to get chloro derivative (**2**), which then coupled with 3-aminoaniline in isopropyl alcohol at 80 °C to get *meta*-phenylenediamine derivative (**3**). Structure of the compound **3** was confirmed by the appearance of $-NH_2$ in the ^1H NMR spectrum of compound **3** around δ 9.5 and a peak at δ 10.5 corresponding to –NH. Compound **3** was then treated

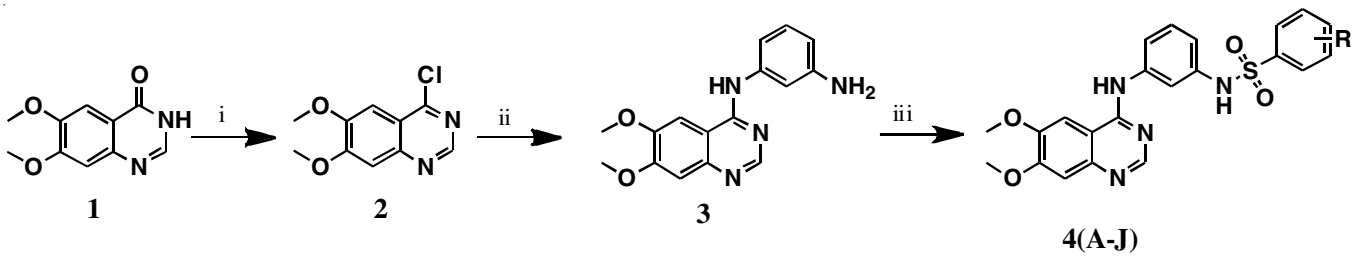

Scheme-I: Synthesis of compounds **4(A-J):** (i) Thionyl chloride, DMF, reflux, 2 h; ii) *meta*-phenylenediamine, Isopropyl alcohol, reflux, 3-4 h; iii) Substituted benzene sulfonyl chlorides, triethyl amine, dichloromethane, 0 °C to room temperature, 4-5 h

with different aryl sulfonyl chlorides in presence of triethylamine in dichloromethane to get crude products **4(A-J)**, which were further purified by using silica gel column. The structure of compounds **4(A-J)** were confirmed by the disappearance of $-NH_2$ peak in the ^1H NMR spectrum of compounds and appearance of –NH peak around δ 10.4. Structures and yields of the compounds are presented in Table-1.

Compound 4G induces cytotoxic effect in EAC cells: The synthesized compounds **4(A-J)** were evaluated for their anti-proliferative activity on EAC cell lines using MTT assay. Cisplatin was used as positive control. All the synthesized compounds significantly inhibited the proliferation of cancer cells in a dose-dependent manner (1-100 μM) after 24 h of incubation. IC_{50} values for the cytotoxic effects of various synthetic compounds **4(A-J)** are shown in Table-1. The compounds **4A**, **4B**, **4C**, **4E**, **4F**, **4G** and **4H** showed good activity with IC_{50} values 27.4 ± 2.14, 18.3 ± 1,94, 24.2 ± 1.91, 22.5 ± 2.13,12.9 ± 2.1, 10.29 ± 1.14 and 14.8 ± 1.91 μM, respectively, whereas the IC_{50} value for cisplatin was 6.4 ± 1.45 μM. These values suggest that the activities of the synthesized compounds are very close to that of the standard cisplatin. Compounds **4A** and **4C** with halogen substituents on phenyl ring at various positions (2,4 and 5) are least active (24.2 ± 1.94 to 27.4 ± 2.14 μM). Activating groups like methoxy, on *para* position of phenyl ring, which release electrons by resonance in **4B** enhanced the activity to 18 ± 1.94 μM. Besides, inductively electron releasing 4-*tert* butyl group in **4E** is less active (22.5 ± 2.13 μM). On the other hand, deactivating group like nitro, irrespective of its position on phenyl ring of compounds **4F-H**, enhanced the activity (10.29 ± 1.14 to 14.8 ± 1.91 μM). Thus, compounds **4F-H** showed 1-2 fold high IC_{50} values compared to that of the standard cisplatin. In particular, the order of activity is 4-nitro (**4G**) > 2-nitro (**4F**) > 3-nitro (**4H**). Compound **4G**, which showed the highest activity (10.29 ± 1.14 μM) was taken for further studies.

Induction of antitumor activity by compound 4G significantly increases survivability of treated mice: We adopted EAC murine model to evaluate the anti-proliferative and pro-apoptotic activity of the compound **4G**. To determine the *in vivo* effect on cell growth, we investigated the effect of **4G** compound on body weight, ascites volume and survivability in the treated and untreated tumor bearing mice. We observed there was a gradual decrease in the body weight (Fig. 1A), ascites volume (Fig. 1B) and there was a significant increase (53 %) in life span of compound **4G** treated mice in comparison with control (Fig. 1C). Decrease in tumor growth also correlates with significant increase in life span. Our lead compound **4G** inhibits the tumor growth and increases survivability of the mice (Fig. 1D). The prolongation of lifespan of compound **4G** treated EAC bearing mice is a very important and reliable criterion.

Compound 4G induces apoptosis in EAC cells: Microscopic examination of cell morphology revealed the characteristic apoptotic features such as cell shrinkage, formation of small blebs and apoptotic bodies in 4G treated cells (Fig. 2A). Cytological analysis showed nuclear condensation when compound **4G** treated cells are stained with acridine orange/ethidium bromide, which is an important feature of apoptosis as compared to the untreated EAC cells (Fig. 2B). Activation

TABLE-1
STRUCTURE, YIELD (%) AND IC_{50} (μM±SD) VALUE OF COMPOUNDS **4(A-J)**

Compd.	Structure	Yield (%)[a]	IC_{50} value (μM)
4A	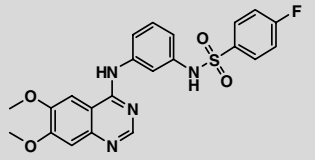	59	27.4±2.14
4B	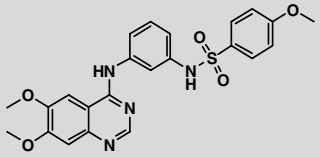	55	18.3±1.94
4C	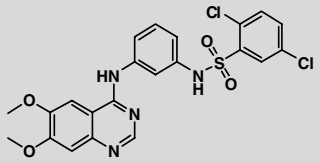	60	24.2±1.94
4D	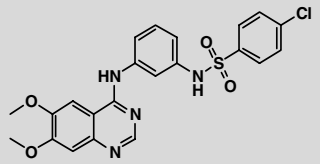	65	NA
4E	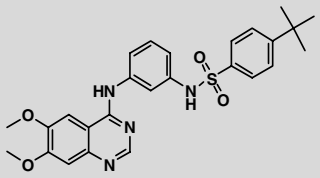	59	22.5±2.13
4F	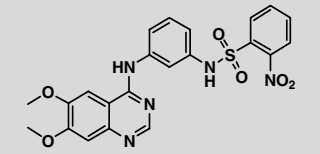	65	12.9±2.1
4G	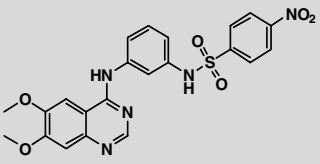	60	10.29±1.14
4H	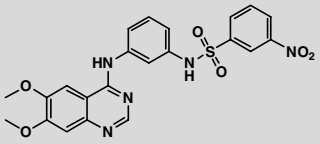	52	14.8±1.91
4I	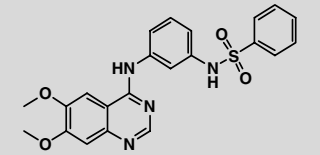	55	NA
4J	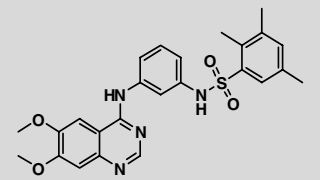	60	NA

NA = Not active; [a]Yield corresponds to the final step of synthesis

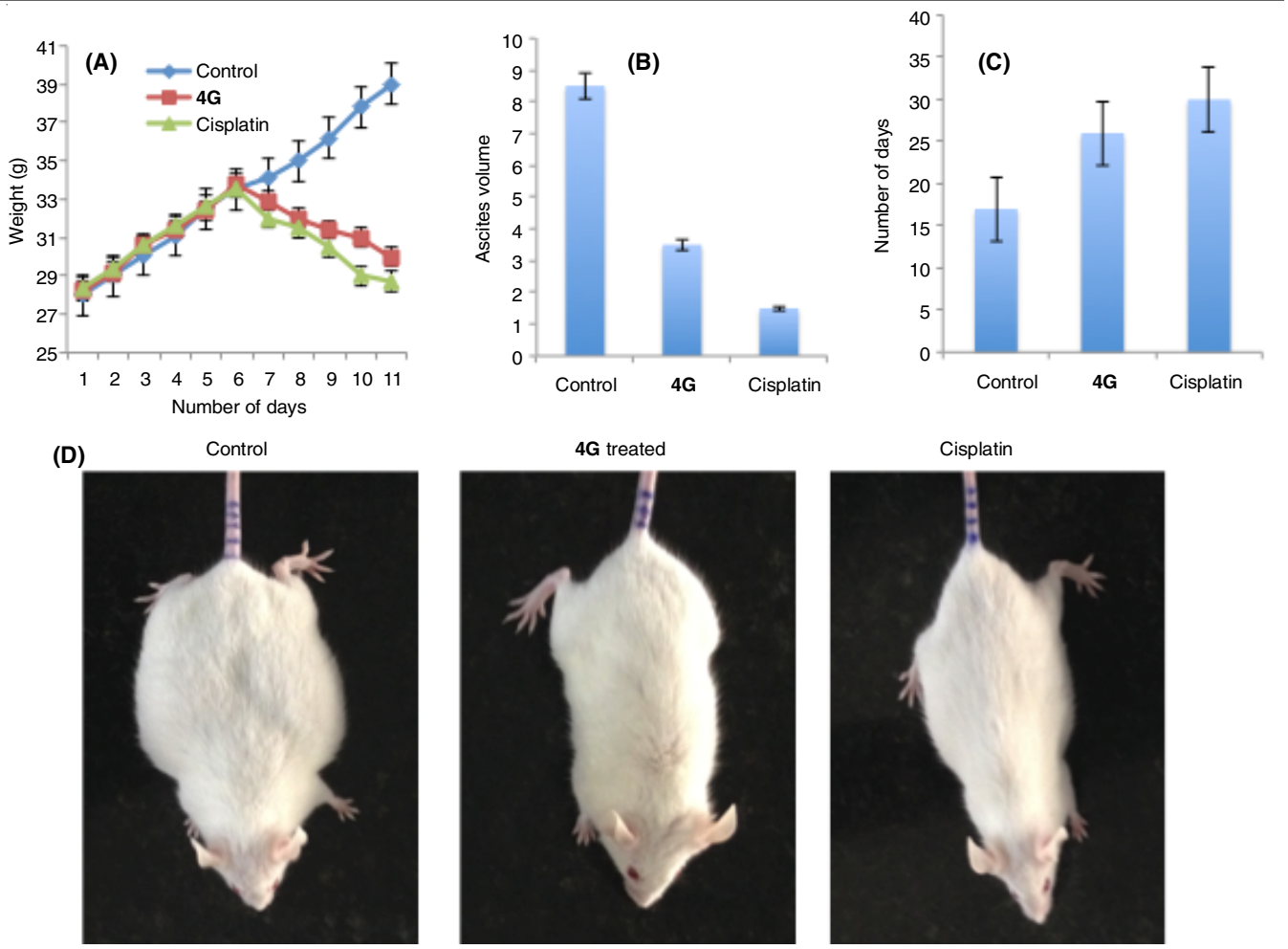

Fig. 1. Compound **4G** inhibit the proliferation of EAC cells. (A) Decrease in the body weight of compound **4G** treated treated mice when compare to control, (B) Compound **4G** decreases the Ascites fluid volume in tumor bearing mice. (C-control, CP-Cisplatin, **4G** treated). (C) Increased Survivability of treated mice when compared to untreated tumor bearing mice. **(D)** Photograph showed the external morphology of tumor bearing control, **4G** treated and cisplatin treated mice

of proteolytic enzymes such as cysteine, serine proteases and proteasomes may correlate with the main apoptotic events includes plasma membrane blebbing, shrinkage of the cytoplasm, dilation of endoplasmic reticulum, nuclear chromatin condensation and DNA fragmentation. The nuclear condensation and formation of apoptotic bodies indicates that the compound **4G** induce apoptosis in treated cells when compared to that of control cells that showed intact nuclear architecture.

Compound 4G inhibits cell viability and induces caspase-3 activation: Trypan blue dye exclusion method was used to determine the cell viability. The result shows a significant decrease in viability of **4G** treated cells when compared to untreated cells (Fig. 3A). Activation of caspase-3 pathway is a hallmark of apoptosis and can be used in cellular assays to quantify activators and inhibitors of the "death cascade". The response is both time and concentration dependent, suggesting that multiple pathways play a role in triggering the caspase-3 activation. To evaluate the effect of compound **4G** in treated cells, a significant proportion of cells were induced to undergo apoptosis through caspase-3 activation and the effects were determined by the flow cytometric analysis. FACS analysis shows that, about 45 % of treated cells with active caspase-3 where as in control it was 2.7 %. Besides, 63 % of cisplatin treated cells showed activated caspase-3. (Fig. 3B).

Compound 4G induced apoptosis is dependent on caspase-3 activation: The appraisal of apoptotic pathway was further carried out by determining the DNA ladder patterns. EAC cells treated with compound **4G** showed characteristics of DNA laddering that had higher apoptotic cells while the DNA of control cells exhibited minimum fragmentation. Cisplatin was used as a positive control (Fig. 4A). The downstream signaling pathway revealed that the activation of caspase-3 in compound **4G** treatment induced EAC cell death. In order to check the involvement of caspase-3 activator of endonuclease, the cells were treated with or without caspase-3-inhibitor (Ac-DEVD-CHO), prior to the treatment with **4G** compounds [30]. The results clearly suggest that, the DNA fragmentation is due to increased endonuclease activity but the Ac-DEVD-CHO, a specific inhibitor of caspase-3 enzyme inhibited the DNA fragmentation (Fig. 4B). DNA degradation and caspase-3 inhibition assays showed that the compound **4G** induce caspase-3 mediated apoptosis in EAC cells.

BAX activation by compound 4G leads to cleavage of PARP in EAC cells: The signaling pathway by which compound **4G** induces apoptosis in EAC cells was depicted by assessing

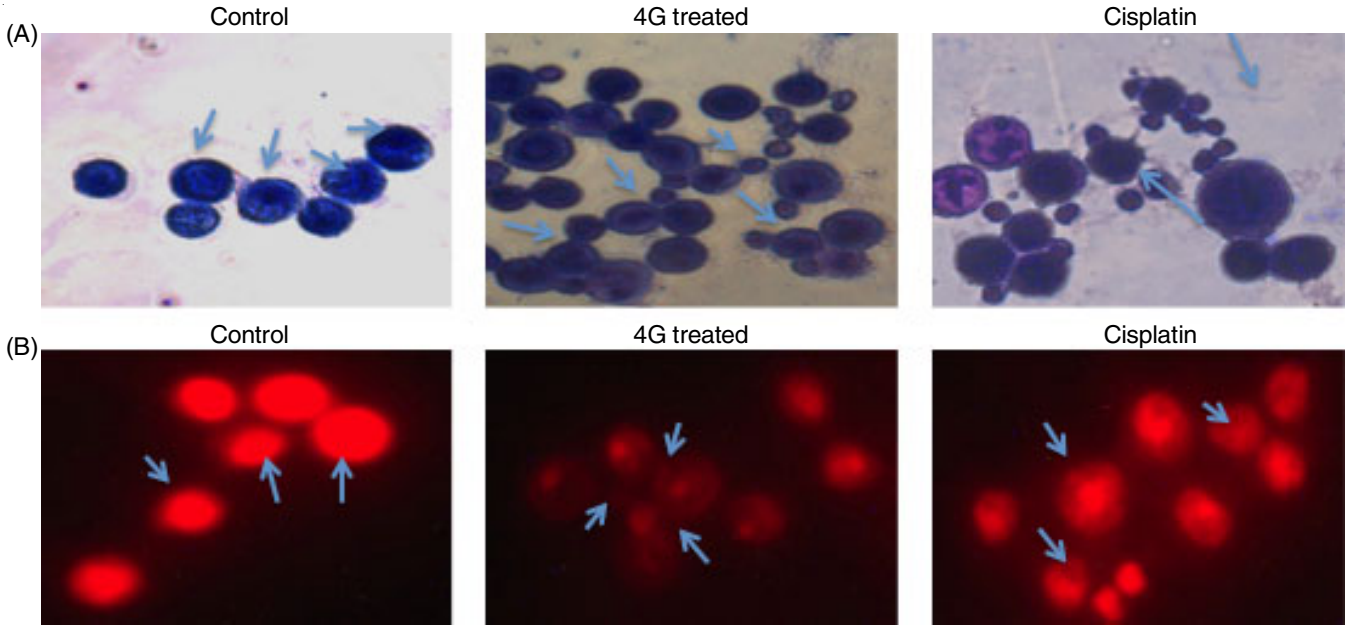

Fig. 2. Changes in the cellular morphology of EAC cells: cells treated with and without compound were stained with Giemsa and acridine orange stain were viewed under microscope and photographed. (A) Compound **4G** treated cells showed morphological changes and formation of apoptotic bodies. (B) Changes in the nuclear morphology of cell in EAC cells of compound **4G** treated mice

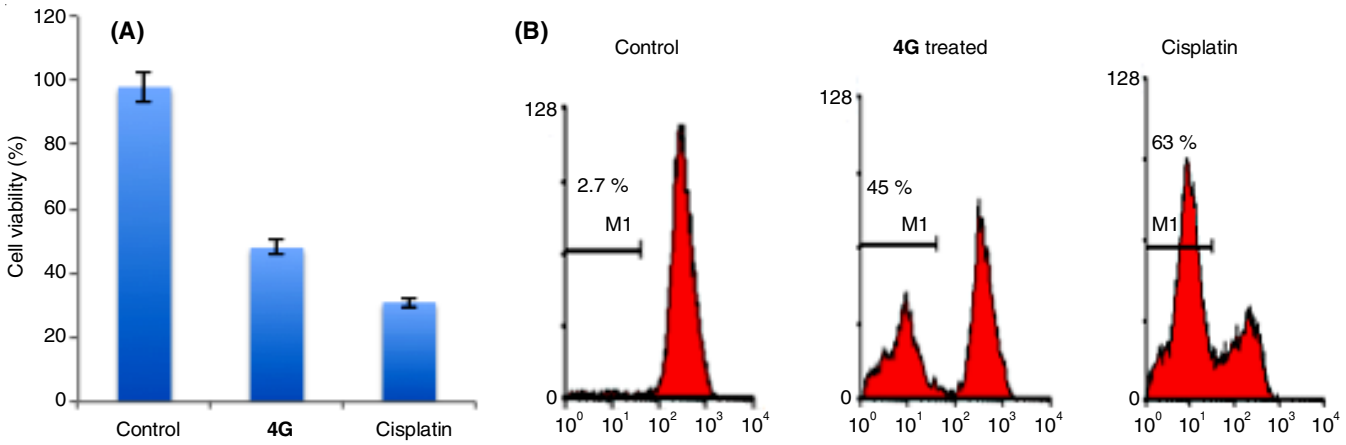

Fig. 3. (A) Compound **4G** reduce the percentage of viable cells, (B) Flow cytometric analysis of apoptosis in EAC cells by **4G** compounds. (C – control, **4G** – quinazoline compound, CP – cisplatin)

the changes in expression levels of apoptotic proteins. Bcl-2 superfamily plays an important role in apoptosis; it acts as activator or inhibitor. Of this, the anti-apoptotic protein Bcl-2 and pro-apoptotic protein BAX play important role in cell death. In mitochondrial pathway, compound **4G** induced apoptosis was investigated by examining the level of Bcl-2 and BAX expression, which are the crucial regulators of the apoptotic pathway using RT-PCR. In the present study, compound **4G** increased mRNA expression level of BAX and reduced level of Bcl-2 was observed (Figs. 5A and 5B). So our data suggest that the compound **4G** may disturb the Bcl-2/BAX ratio and leads to apoptosis of EAC cells. Activation of caspase was determined by the cleavage of specific caspase substrates. Activation of caspase-3 results in the cleavage of key proteins such as poly-ADP-ribose polymerase (PARP), lamins and inhibitor of caspase-activated DNase in downstream cascade, resulting in programmed cell death. The nuclear enzyme PARP is cleaved by executioner caspase-3 and -7 [35,36]. The western blot data clearly revealed the cleavage of PARP protein in treated cells where as in control cells it was intact (Fig. 5C). Cisplatin treated cells served as a positive control and were found to have effectively down regulated the expression of Bcl-2, BAX and PARP cleavage. This provides a strong indication that compound induces apoptosis in EAC cells.

Conclusion

In conclusion, the synthesized novel quinazoline derivatives have shown anticancer potential against EAC cells. Compound **4G** possess the capability of inducing mitochondrial pathway in EAC cells, which is well regulated by caspase enzymes. Moreover, the active role of mitochondrial dependent pathway has been studied and was further confirmed by increasing BAX pro-apoptotic protein level, activation of caspase-3 and cleavage of PARP protein by caspase-3 proteins. Our findings strongly suggest that the anticancer and proapoptotic potential of compound **4G** can be used as lead for developing therapeutic agent for treating cancer.

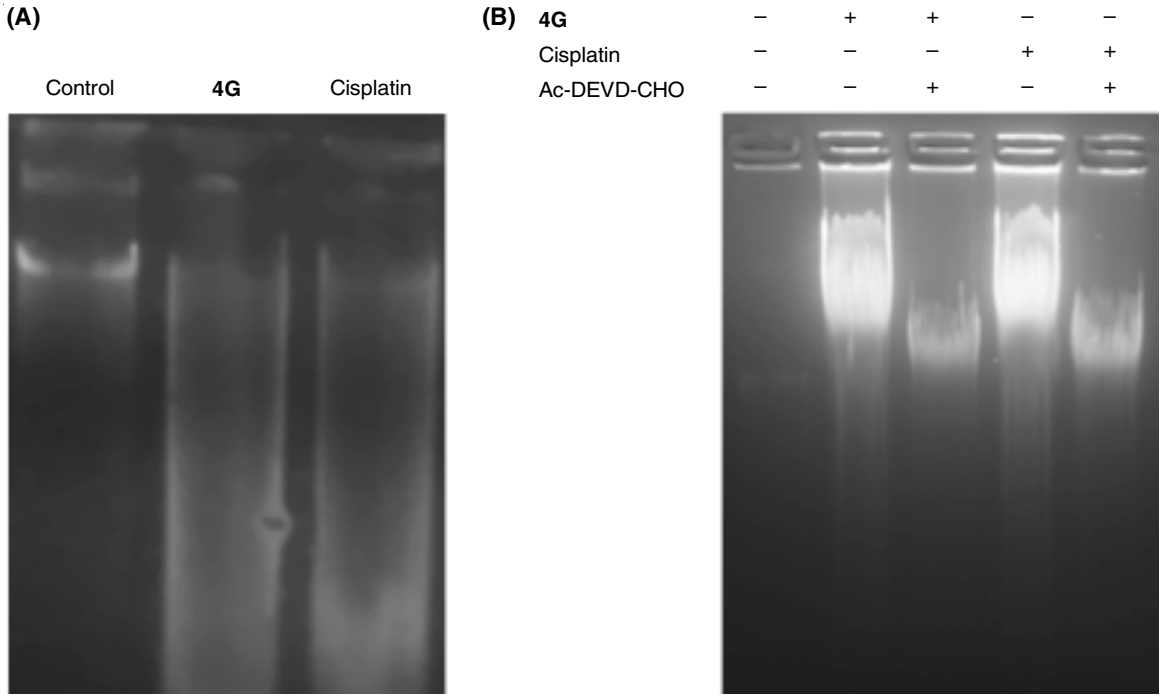

Fig. 4. (A) DNA fragmentation assays, (B) Effect of caspase-3-inhibitor on compound **4G** induced DNA fragmentations

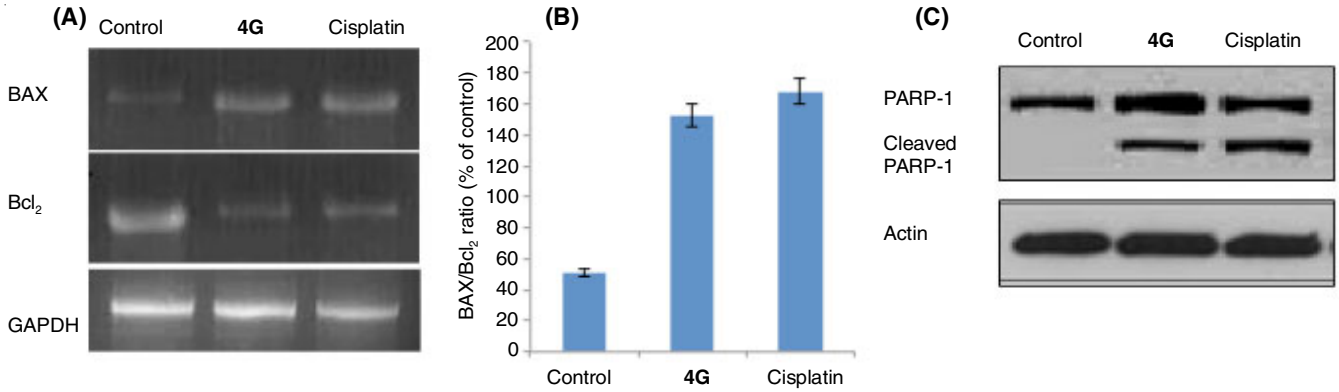

Fig. 5. (A & B) RT-PCR data showing the expression levels of BAX and Bcl_2 genes. (C) Compound **4G** induce the expression of cleaved PARP in EAC cells (C – control, CP – cisplatin, **4G** – quinazoline compound

ACKNOWLEDGEMENTS

One of the authors, Shankar Jayaram acknowledge thankfully for the financial support provided by UGC, Govt. of India (Sanction No. UGC41-576/2012/(SR) and VGST, Govt. of Karnataka under CISEE programe (GRD No. VEST/CISEE/197). Dated 18-july-2012. Another author, Doddakunche Shivaramu Prasanna acknowledges thankfully SERB, DST, Govt. of India for financial assistance (Sanction No. YSS/2015/001930). Finally, the authors also thank Central Animal Facility, Department of Zoology, University of Mysore, Mysore, India for providing the animal facility.

REFERENCES

1. H. Sun and Y. Wang, *Physiology*, **27**, 43 (2012); https://doi.org/10.1152/physiol.00034.2011.
2. J. Plati, O. Bucur and R. Khosravi-Far, *Integr. Biol.*, **3**, 279 (2011); https://doi.org/10.1039/c0ib00144a.
3. S. Elmore, *Toxicol. Pathol.*, **35**, 495 (2007); https://doi.org/10.1080/01926230701320337.
4. J.F. Kerr, A.H. Wyllie and A.R. Currie, *Br. J. Cancer*, **26**, 239 (1972); https://doi.org/10.1038/bjc.1972.33.
5. S. Fulda and K.M. Debatin, *Curr. Cancer Drug Targets*, **4**, 569 (2004); https://doi.org/10.2174/1568009043332763.
6. F.H. Igney and P.H. Krammer, *Nat. Rev. Cancer*, **2**, 277 (2002); https://doi.org/10.1038/nrc776.
7. K.C. Zimmermann, C. Bonzon and D.R. Green, *Pharmacol. Ther.*, **92**, 57 (2001); https://doi.org/10.1016/S0163-7258(01)00159-0.
8. K.C. Zimmermann and D.R. Green, *J. Allergy Clin. Immunol.*, **108**, S99 (2001); https://doi.org/10.1067/mai.2001.117819.
9. C. Toruno, S. Carbonneau, R.A. Stewart and C. Jette, *Plos One*, **9**, e88151 (2014); https://doi.org/10.1371/journal.pone.0088151.
10. M. Kruidering and G.I. Evan, *IUBMB Life*, **50**, 85 (2000); https://doi.org/10.1080/713803693.
11. M. Los, M. Mozoluk, D. Ferrari, A. Stepczynska, C. Stroh et al., *Mol. Biol. Cell*, **13**, 978 (2002); https://doi.org/10.1091/mbc.01-05-0272.
12. H.K. Lorenzo and S.A. Susin, *FEBS Lett.*, **557**, 14 (2004); https://doi.org/10.1016/S0014-5793(03)01464-9.

13. H.H. Ahmed, G.A. Elmegeed, E.-S.M. El-Sayed, M.M. Abd-Elhalim, W.G. Shousha and R.W. Shafic, *Eur. J. Med. Chem.*, **45**, 5452 (2010); https://doi.org/10.1016/j.ejmech.2010.09.017.
14. K. Magyar, L. Deres, K. Eros, K. Bruszt, L. Seress, J. Hamar, K. Hideg, A. Balogh, F. Gallyas Jr., B. Sumegi, K. Toth and R. Halmosi, *Biochim. Biophys. Acta*, **1842**, 935 (2014); https://doi.org/10.1016/j.bbadis.2014.03.008.
15. Y. Rojas-Aguirre, F. Hernandez-Luis, C. Mendoza-Martínez, C.P. Sotomayor, L.F. Aguilar, F. Villena, I. Castillo, D.J. Hernandez and M. Suwalsky, *Biomembranes*, **1818**, 738 (2012); https://doi.org/10.1016/j.bbamem.2011.11.026.
16. M.N. Noolvi, H.M. Patel, V. Bhardwaj and A. Chauhan, *Eur. J. Med. Chem.*, **46**, 2327 (2011); https://doi.org/10.1016/j.ejmech.2011.03.015.
17. A.S. El-Azab, M.A. Al-Omar, A.A.-M. Abdel-Aziz, N.I. Abdel-Aziz, M.A.-A. El-Sayed, A.M. Aleisa, M.M. Sayed-Ahmed and S.G. Abdel-Hamide, *Eur. J. Med. Chem.*, **45**, 4188 (2010); https://doi.org/10.1016/j.ejmech.2010.06.013.
18. M.T. Conconi, G. Marzaro, L. Urbani, I. Zanusso, R. Di Liddo, I. Castagliuolo, P. Brun, F. Tonus, A. Ferrarese, A. Guiotto and A. Chilin, *Eur. J. Med. Chem.*, **67**, 373 (2013); https://doi.org/10.1016/j.ejmech.2013.06.057.
19. S. Ravez, A. Barczyk, P. Six, A. Cagnon, A. Garofalo, L. Goossens and P. Depreux, *Eur. J. Med. Chem.*, **79**, 369 (2014); https://doi.org/10.1016/j.ejmech.2014.04.007.
20. F. Zhao, Z. Lin, F. Wang, W. Zhao and X. Dong, *Bioorg. Med. Chem. Lett.*, **23**, 5385 (2013); https://doi.org/10.1016/j.bmcl.2013.07.049.
21. M.L.C. Barbosa, L.M. Lima, R. Tesch, C.M.R. Sant'Anna, F. Totzke, M.H.G. Kubbutat, C. Schächtele, S.A. Laufer and E.J. Barreiro, *Eur. J. Med. Chem.*, **71**, 1 (2014); https://doi.org/10.1016/j.ejmech.2013.10.058.
22. L. Zhang, Y. Yang, H. Zhou, Q. Zheng, Y. Li, S. Zheng, S. Zhao, D. Chen and C. Fan, *Eur. J. Med. Chem.*, **102**, 445 (2015); https://doi.org/10.1016/j.ejmech.2015.08.026.
23. Y. Pu, D. Cao, C. Xie, H. Pei, D. Li, M. Tang and L. Chen, *Biochem. Biophys. Res. Commun.*, **462**, 288 (2015); https://doi.org/10.1016/j.bbrc.2015.04.111.
24. V. Chandregowda, G. Venkateswara Rao and G. Chandrasekara Reddy, *Org. Process Res. Dev.*, **11**, 813 (2007); https://doi.org/10.1021/op700054p.
25. S. Priyanka, K.S. Balaji, K.T. Chandrashekar, K.S. Rangappa and J. Shankar, *Int. J. Appl. Biol. Pharm. Technol.*, **6**, 680 (2015).
26. A. Kumar, S.S. D'Souza, S. Tickoo, B.P. Salimath and H.B. Singh, *Integr. Cancer Ther.*, **8**, 75 (2009); https://doi.org/10.1177/1534735408330716.
27. G. Srinivas, R.J. Anto, P. Srinivas, S. Vidhyalakshmi, V.P. Senan and D. Karunagaran, *Eur. J. Pharmacol.*, **473**, 117 (2003); https://doi.org/10.1016/S0014-2999(03)01976-9.
28. B.R. Vijay Avin, P. Thirusangu, V. Lakshmi Ranganatha, A. Firdouse, B.T. Prabhakar and S.A. Khanum, *Eur. J. Med. Chem.*, **21**, 211 (2014); https://doi.org/10.1016/j.ejmech.2014.01.050.
29. M. Belakavadi, B.T. Prabhakar and B.T. Salimath, *Biochem. Biophys. Res. Commun.*, **335**, 993 (2005); https://doi.org/10.1016/j.bbrc.2005.07.172.
30. C. Anil Kumar, S. Jayarama, Basappa, B.P. Salimath and K.S. Rangappa, *Invest. New Drugs*, **25**, 343 (2007); https://doi.org/10.1007/s10637-006-9033-4.
31. M. Belakavadi and B.P. Salimath, *Mol. Cell. Biochem.*, **273**, 57 (2005); https://doi.org/10.1007/s11010-005-7717-2.
32. A.H. Wyllie, *Nature*, **284**, 555 (1980); https://doi.org/10.1038/284555a0.
33. S. Agarwal and S. Gupta, *J. Immunol.*, **160**, 1627 (1998).
34. L.-C. Li, S. Jayarama, L. Ganesh, L. Qian, J. Rotmensch, A.V. Maker and B.S. Prabhakar, *Am. J. Obstet. Gynecol.*, **205**, 362.e12 (2011); https://doi.org/10.10.1016/j.ajog.2011.05.035.
35. G. de Murcia and J.M. de Murcia, *Trends Biochem. Sci.*, **19**, 172 (1994); https://doi.org/10.1016/0968-0004(94)90280-1.
36. Y.A. Lazebnik, S.H. Kaufmann, S. Desnoyers, G.G. Poirier and W.C. Earnshaw, *Nature*, **371**, 346 (1994); https://doi.org/10.1038/371346a0.